Medical Engineering and Physics 71 (2019) 91–97

Contents lists available at ScienceDirect

Medical Engineering and Physics

journal homepage: www.elsevier.com/locate/medengphy

The effect of acute glutamate treatment on the functional connectivity and network topology of cortical cultures

Yao Han[a,b,1], Huimin Zhu[a,1], Yuwei Zhao[a], Yiran Lang[a], Hongji Sun[a], Jiuqi Han[a], Lubin Wang[c], Changyong Wang[a], Jin Zhou[a,*]

[a] Department of Neural Engineering and Biological Interdisciplinary Studies, Institute of Military Cognition and Brain Sciences, Academy of Military Medical Sciences, Beijing, PR China
[b] Stem Cell and Tissue Engineering Lab, Institute of Health Service and Transfusion Medicine, Beijing, PR China
[c] Cognitive and Mental Health Research Center, Beijing Institute of Basic Medical Sciences, Beijing, PR China

ARTICLE INFO

Article history:
Received 25 December 2018
Revised 25 June 2019
Accepted 5 July 2019

Keywords:
Neuronal culture
Graph theory
Connectivity
Microelectrode arrays
Glutamate

ABSTRACT

Microelectrode arrays (MEAs) allow the investigation of the pharmacological and toxicological effects of chemicals on cultured neuronal networks. Understanding the functional connections between neurons and the resulting neuronal networks is important for evaluating drugs that affect synaptic transmission. Therefore, we acutely treated a mature cultured neuronal network on MEAs with accumulating amounts of glutamate and recorded their altered electrophysiology. Subsequently, a cross-covariance analysis was applied to process the spiking activity in the network and to evaluate the connections between neurons. Finally, graph theory was used to assess the functional network properties under acute glutamate treatment. Our data demonstrated that glutamate increased the similarity, connectivity weight, density, and largest-component size of the functional network. In addition, the small-world network topology was altered after glutamate treatment. Our results indicate that the graph theory can advance our understanding of the pharmacological significance of neurotransmitters on neuronal networks.

1. Introduction

The brain is a complex organ, and the available methods for experimentation are limited. Culturing neuronal networks on microelectrode arrays (MEAs) has been used as a simplified model to simulate synaptic formation and electrical connectivity and to study neuronal networks *in vitro*. These cultured networks resemble the neuronal networks that are present in the brain *in vivo* and in brain slice preparations. Furthermore, such networks spontaneously produce bursts of synchronized firing events that are termed "network bursts," typically observed after 14 d *in vitro* (DIV) [10,14,15]. During network bursts, a large proportion of neurons fire trains of action potentials within a short period, in the order of hundreds of ms [11,17,18], and most of the neurons within a network interact with other within-network neurons. Studies have broadly analyzed and characterized the statistics of the neuronal-spike trains of a network burst to interpret the significance of the network-burst activity [3,6,27,31]. Network bursts are composed of subgroups with distinct spatiotemporal correlation patterns [22], and the inhibitory antagonism [2] or architecture [19] of cultures evoke different network bursts. However, more data are needed to understand how neurons are organized into a neuronal network, how information is transmitted with in a neuronal network, and how external stimulation affects the organization of the functional network.

Graph theory provides tools for the study of functional neuronal networks as a complex system, and presents new hypotheses about the interactions between neurons. In 2007, Bettencourt et al. [4] reported that the mature functional neuronal network had a small-world property (most of the nodes were not connected directly but could communicate with few intermediate relay steps). In 2012, Downes et al. [9] discovered that neuronal networks display a random network topology at the initial stage of culture; however, as the neuronal cultures matured, the small-world network topology dominated and several "hub" nodes (highly connected nodes) appeared. In 2015, Schroeter et al. [21] found that rich-club topology (nodes rich in connections tend to form strongly interconnected clubs) emerges during the development of neuronal cultures. By examining the network as a whole system, these studies provide a new understanding of the function of neuronal networks that includes the functional structures of neurons and their dynamic properties.

* Corresponding author.
E-mail address: sisun819@yahoo.com (J. Zhou).
[1] These authors contributed equally to this work.

https://doi.org/10.1016/j.medengphy.2019.07.007
1350-4533/

To evaluate the effects of neuroactive substances on neuronal networks, the importance of investigating the whole network properties is increasingly being recognized. Glutamate [23] and 4-aminopyridine/bicuculline [29] have been used to construct neuronal cultures as models of epilepsy or ischemia for exploring the topologies of functional networks. These drugs can change the small-world network topology and connection patterns.

In the present study, we used the excitatory neurotransmitter glutamate to acutely treat cultured cortical networks. Network functional connectivity was reconstructed by calculating the cross-covariation during synchronous network bursts. In addition, we examined the graph theory properties of the resulting functional network. Our results reveal the effect of acute glutamate exposure on the functional connectivity of neuronal cultures.

2. Materials and methods

2.1. Animals

We purchased gestational female Sprague-Dawley rats from the Experimental Animal Center, Academy of Military Medical Science (Beijing, PRC). Each rat was individually housed in a cage with water and food supplied ad libitum in a room at a constant temperature of 24 ± 2 °C with a 12:12 h light-dark cycle. Five rats were used for the isolation of neurons. One rat was not pregnant.

2.2. The recording system and MEAs

The recording system was produced as reported previously [33] and included a 32-channel amplifier, a NI USB-6259 data-acquisition card, and custom-developed recording software by LabVIEW (National Instruments, USA). Our custom-made MEAs had 59 indium tin oxide (ITO)–platinum microelectrodes and a large-area grounding electrode. Our MEAs utilize electroplated fuzzy gold as an intermediate layer and have better platinum black adhesion to ITO microelectrodes. The microelectrode diameter was 30 µm, and the inter-electrode distance was 200 µm. More details are available in previously published work [25].

2.3. Neuronal cell culture on MEAs

On gestational day 16–18, the cerebral cortices were isolated from embryonic Sprague-Dawley rats weighing 250–300 g, and cut into pieces using curved scissors. The cortical tissue pieces were incubated in 5 mL of 0.25% trypsin (Sigma-Aldrich, St Louis, MO, USA) for 30 min at 37 °C for cell dissociation. The dissociated cells were collected in Dulbecco's Modified Eagle's Medium (DMEM) (Sigma-Aldrich) with 10% equine serum (Hyclone, GE Healthcare, Chicago, IL, USA) and 10% fetal calf serum (Hyclone). Before plating the cells, MEAs were precoated with poly-L-lysine (Sigma-Aldrich, 0.1 mg/mL), and then with Matrigel (Sigma-Aldrich) on the day of culturing (0.2 mg/mL; Sigma). MEAs were seeded with 1,000,000 cells in 1 mL of culture media at a density of 3000 cells /mm^2. After cells adhered onto the MEAs, the culture medium was replaced with DMEM and 10% equine serum (Hyclone) and half of the medium was renewed every 2 d

2.4. Glutamate treatment protocol and electrophysiology recordings

The MEAs with cultured neurons were exposed to the excitatory neurotransmitter glutamate (Sigma-Aldrich). The treatment of cultured neurons with glutamate was performed as reported previously [8]. Briefly, half of the culture medium was replenished 48 h before experimentation to stabilize the cultures. At 21 DIV, the glutamate stock solutions were prepared and diluted with deionized water to produce a concentration series for experimentation (glutamate concentrations: 5 µM, 10 µM, 15 µM, 20 µM, and 25 µM; volume, 1 mL).In total, 200 µL of culture medium incubating the MEAs was mixed with 1 µL of each glutamate dilution, and then was carefully returned to the original MEA culture medium to minimize any osmotic or hydrodynamic stress.

The activities of the cultured neuronal network were stabilized for 10 min before each recording. Subsequently, their spontaneous activity was recorded for 10 min. All of the recording experiments were performed at 37 °C with 5% CO_2 in a humidified incubator.

2.5. Spike detection

An Offline Sorter (Plexon Inc., Dallas, TX, USA) was used to perform spike detection. A band-pass filter (200–5000 Hz) was used to remove the baseline shifts and high-frequency noise. The threshold for spike detection was set at 5 standard deviations (SD) from the background signal.

2.6. Burst detection

Burst definition was previously defined [5], and burst detection was performed using Neuroexplorer (NexTechnologies Inc., Woodway, TX, USA). Briefly, spike trains that have minimum burst interval of 0.1 s, minimum burst duration of 0.1 s, and minimum 5 spikes per burst were considered as bursts in a single channel.

2.7. Network burst detection

Network bursts are the synchronous activity of the neuronal culture, and provide information about the interaction between neurons. To detect network bursts, we used a previously reported algorithm that was based on the SIMMUX algorithm included in MEABench [30]. A network burst was required to contain at least 4 channels in 250 ms, and each contained an electrode recording of at least 3 spikes in 100 ms. The network-burst onset and end were defined as the timestamp of the first and last spike in the network burst, respectively. To assess interactions between the neuronal units among all electrodes, "tiny" network bursts were excluded, and only the network bursts in which at least 8 electrodes (25%) were activated (at least 3 spikes in 100 ms) were selected to determine connectivity.

2.8. Cross-covariance method for connection determination

A functional connectivity approach is generally used to describe the interactions within the neuronal activity that has been recorded from multiple sites [1]. Various methods have been used to evaluate the interaction within a cultured neuronal network [1,4,9,16,23,24,30], and the functional connectivity approach was designed to characterize the function of a cultured neuronal network. However, there is no gold-standard method for the optimal estimation of neuronal functional connectivity.

We used a functional-connectivity approach, as previously reported, with a small modification [9]. Briefly, cross-covariance sequence $\Phi_{xy}(m)$ was calculated between spike timestamps of two channels during the network burst, and disdescribed as follows:

$$\Phi_{xy}(m) = E\{(x_{n+m} - \mu_x)(y_n - \mu_y)\}$$

where $\Phi_{xy}(m)$ represents the similarity between vector x and vector y after vector x shifts m time bins, E{} is the expected value operator and μ_x, μ_y are the mean values of the bin value. In our study, vector x or y represents a vector that collects the number of spikes as a slipping time bin (10 ms) during a network burst of one channel.

However, the cross-covariance value may increase with the firing rate [7]. Therefore, a functional connection driven from a cross-covariance value may appear by chance. We applied a shuffling method [26,28] to compare the difference between the real neuronal activity and randomized surrogate neuronal activity to distinguish the real neuronal functional connection from the functional connection detected by chance. Briefly, we used randomized neuronal activity as surrogate to calculate the cross-covariance sequence, and repeated this step 100 times. In addition, the cross-covariance of the real neuronal activity was normalized using a z-score to compare the difference between the cross-covariance value of the real neuronal activity and 100 surrogates. The z-score value Z was computed as follows:

$$Z(m) = \frac{\Phi_{xy}(m) - \left\langle \Phi^{S}_{xy}(m) \right\rangle}{\delta^{S}_{xy}}$$

where δ^{S}_{xy} is the SD of the surrogate values $\Phi^{S}_{xy}(m)$. $Z_{max} = \max(Z(m))(m \neq 0)$ was used as the connectivity weight.

During a network burst, we could have 32 vectors at most. Based on the method described above, we could obtain a 32×32 connectivity weight matrix at each network burst. In our study, a connection was determined using 2 threshold schemes. For basic functional connectivity metrics (i.e., degree and network density), the networks were determined across a range of absolute thresholds (0.05–1.0, in steps of 0.05). For complex topological metrics (i.e., small-worldness), the networks were determined across a range of proportional thresholds (2–40% of maximum network density, in steps of 2%), and then the largest connected components were used to compute the small-worldness.

2.9. Graph metrics

The functional network in our paper was evaluated using the graph theory and the Brain Connectivity Toolbox [20]. The calculated metrics are described in detail bellow.

The upper triangle of the 32×32 cross-covariance matrix was used to construct a vector from a burst, and was similarly estimated using pairwise Spearman correlations between any two network-bursts in the same recording episode. The connection strength of a functional network was defined as the mean of all connection weights (calculated separately for each network burst). Network density was the percentage of realized connections. The degree was defined as the number of connections linked to each node, and 0° corresponded to a node that had no connections. The small-worldness [12,32] described whether a network had a small-world organization or not. If the ratio of the $C^{*}L_{random}/C_{random}{}^{*}L$ was lower than 1, then the network had a small-world organization, where C_{random} and L_{random} represent the average clustering coefficient and average path length of a set of randomly rewired surrogate graphs with the same size and degree of distribution as the original network (100 iterations).

2.10. Statistical analysis

All data are expressed as the mean ± standard error of mean (SEM). SAS software, version 9.0 (SAS Institute, Cary, NC, USA) was used to perform the statistical analyses. The results for each glutamate treatment concentration were compared using a one-way ANOVA with a Tukey's studentized range (honestly significant difference) test and a two-way ANOVA with a Bonferroni post-hoc test. A value of $p < 0.05$ was considered significant.

3. Results

The experiments were carried out using a MEA system built in-house (Fig. 1A) and MEAs (Fig. 1B). Mixed cortical primary neuronal and astroglial cultures were isolated from embryonic day 18 Sprague-Dawley rats, seeded on MEA chips, and developed into mature neuronal networks (Fig. 1C). At 21 DIV, we added glutamate to the cortical neurons as showed in Fig. 1D, recorded the neuronal activities, and analyzed changes in functional connectivity (Fig. 1E).

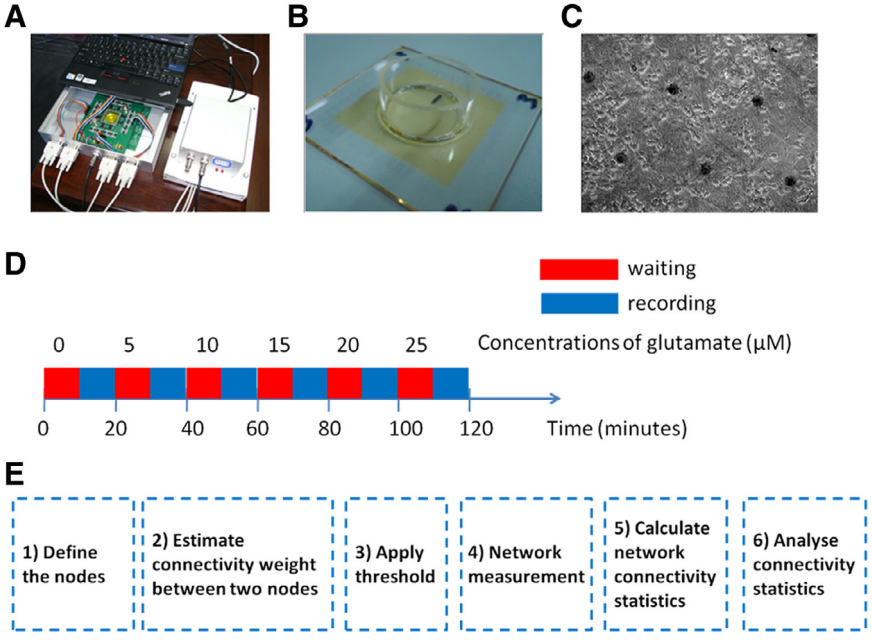

Fig. 1. The experimental setup and procedure: (A) A custom-made microelectrode array (MEA) system; (B) A custom-made MEA; (C) Typical cortical neuronal network cultured on a MEA at 14 days *in vitro*; (D) Glutamate was added to the culture medium at increasing concentrations; (E) Functional connectivity analysis protocol. All cultures were stabilized for 10 min before recording.

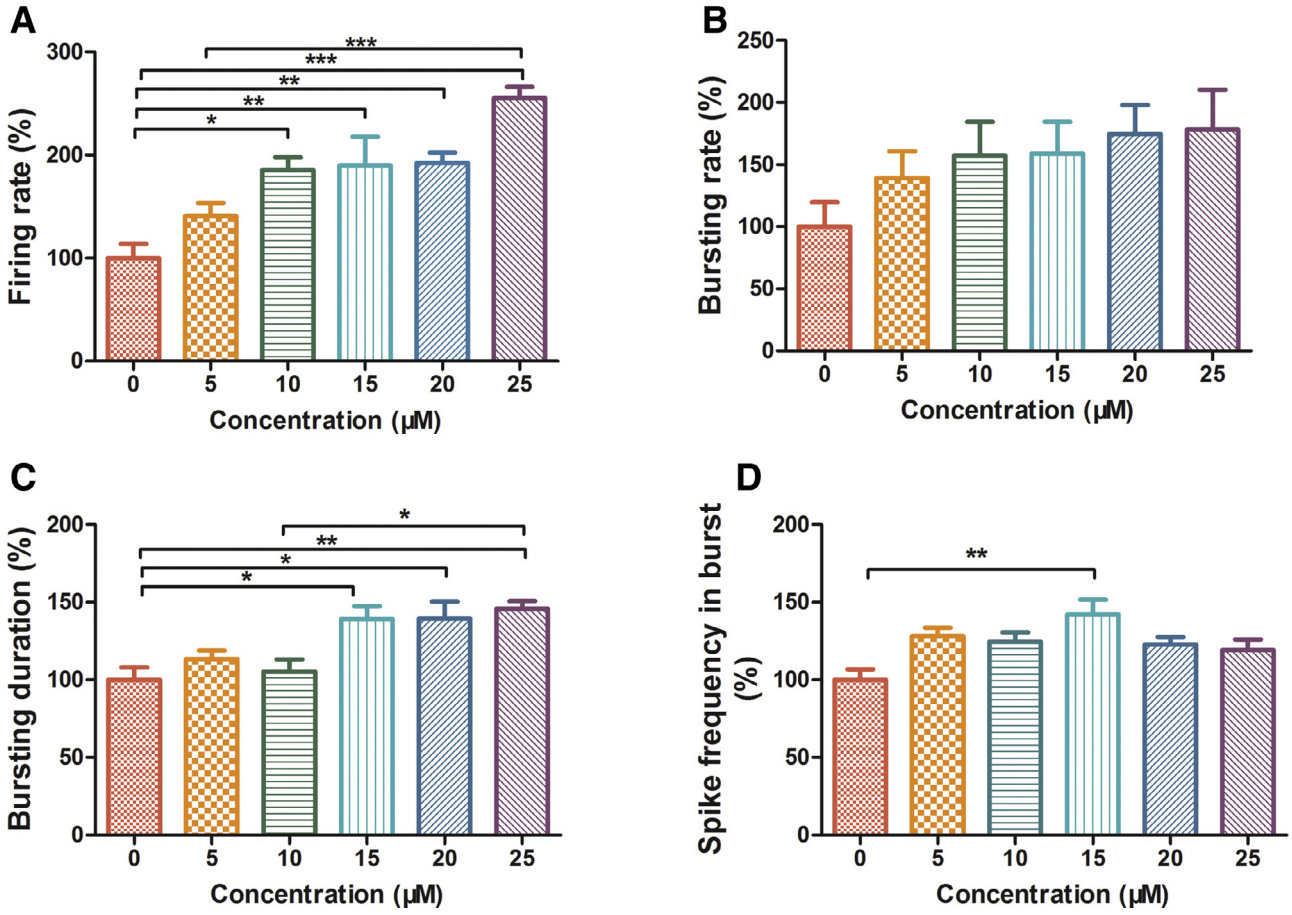

Fig. 2. The change in activity parameters after acute treatment of cortical neuronal cultures with increasing doses of glutamate: (A) Firing rate; (B) Bursting rate; (C) Burst duration; (D) Spike frequency in burst. $^{*}p < 0.05$, $^{**}p < 0.01$, $^{***}p < 0.0001$. Data are expressed as means ± standard error of means.

3.1. The spiking activity of the cultured neuronal network under acute glutamate treatment

At 21 DIV, the neuronal activities became highly synchronized and showed the typical bursting and spiking pattern. To explore the effect of acute glutamate treatment, 4 MEAs were used, and glutamate was added to the neuronal networks in cumulative concentrations (5, 10, 15, 20, and 25 μM).Neuronal activity was recorded for each concentration of glutamate.

Statistical analysis performed on the different neuronal-activity parameters (i.e., firing rate and burst duration, Fig. 2A and Fig. 2C) indicated that the activity significantly increased at high concentrations of glutamate (i.e., 15–25 μM). The spike frequency of bursts was dependent on the glutamate concentrations ($F = 4.153$, $p = 0.0114$, Fig. 2D), and the spike frequency for bursts that occurred after glutamate treatment at concentrations up to 15 μM was significantly different. However, the change in the bursting rate after glutamate treatment at concentrations up to 25 μM, was overall negligible (Fig. 2B).

3.2. The network-burst dynamics of neuronal cultures under acute glutamate treatment

The typical network-burst activities at baseline (0 μM) and after 25 μM glutamate treatment are illustrated in raster plots (Fig. 3A and 3B, respectively). Under 25 μM glutamate treatment, neuronal cultures displayed more spikes in a network burst. The network-burst rate was significantly increased after treatment with 20 μM and 25 μM glutamate. All 600 signals were used to detect the network burst, and the results were considered for further analysis.

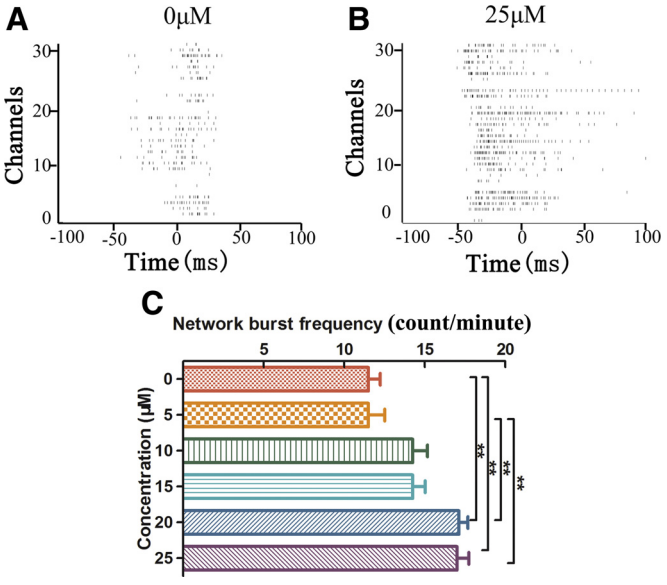

Fig. 3. The network-burst dynamics under glutamate treatment: a raster plot of network bursts under (A) 0 μM and (B) 25 μM glutamate treatment; C, network burst frequency under different concentrations of glutamate treatment.$^{**}p < 0.01$. Data are expressed as means ± standard error of means.

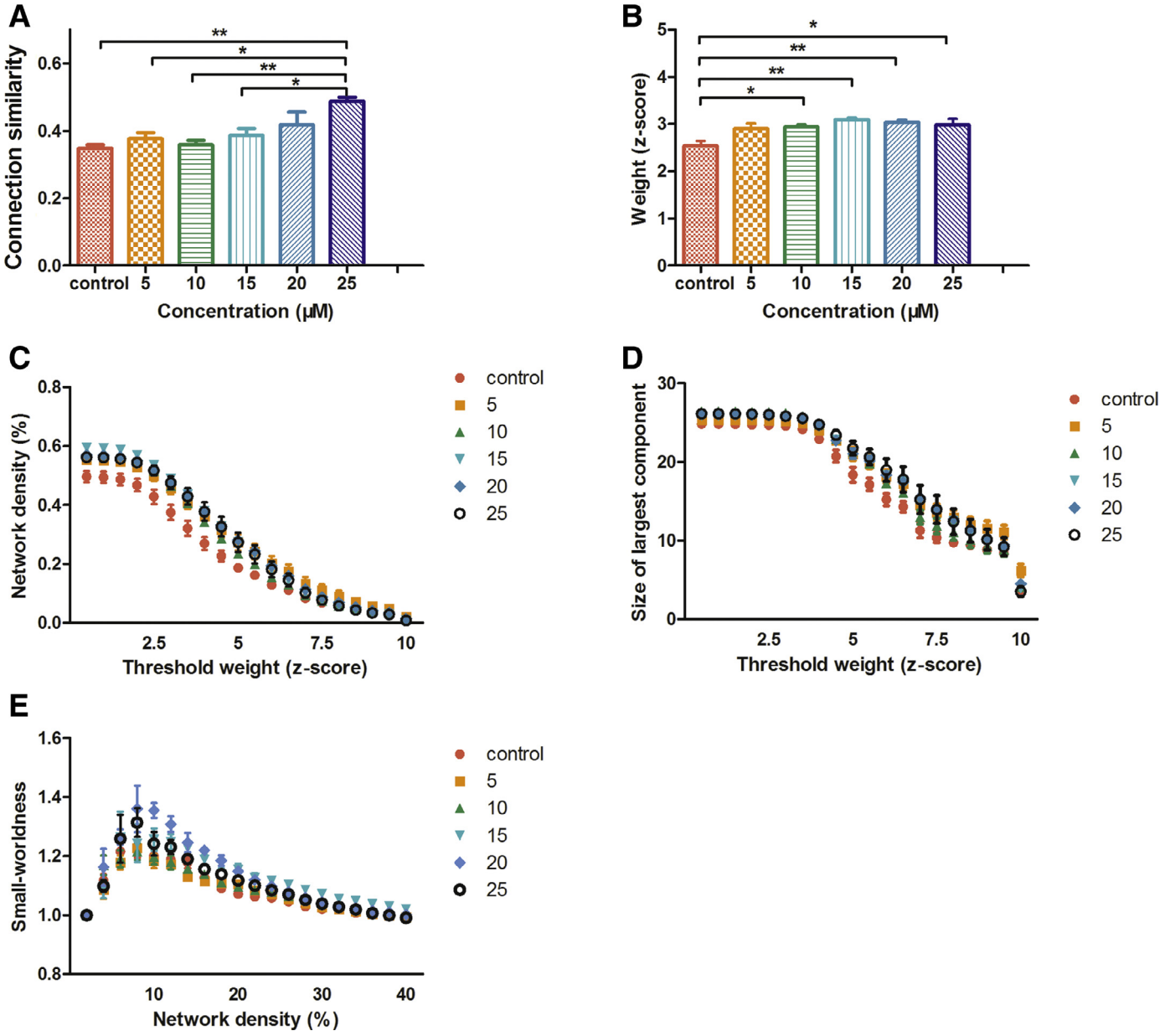

Fig. 4. Increasing concentrations of glutamate induced changes in functional connectivity and network metric of cultured cortical networks: (A) Functional connectivity varied across network bursts within a recording episode; (B) Functional connectivity strength of neuronal cultures under 10, 15, 20, and 25 μM of glutamate increased compared to the control. Network metrics, including the network density (C), size of the largest component (D), and small-worldness (E) were compared in each concentration of acute glutamate treatment. $^{*}p < 0.05$, $^{**}p < 0.01$. Data are expressed as means ± standard error of the means.

3.3. Network topology following acute glutamate treatment

To describe the changes in functional connectivity that were induced by glutamate exposure, we estimated the lagged inter-channel cross-covariance over each network burst for each concentration of glutamate. Next, a shuffling procedure [26,28] was used to compute the connectivity weight between any two nodes. Finally, we constructed a weight matrix to represent the connectivity of a network. The spatiotemporal structure of functional connectivity, which was estimated using pairwise Spearman correlations between all edge weights across 50 randomly selected network bursts (for each recording), suggested a weak similarity (0.3–0.6) among all cultures. Notably, the similarity increased with glutamate concentration ($F = 6.054$, $p = 0.0019$, Fig. 4A). Compared with the baseline condition (0 μM), the application of glutamate enhanced functional connectivity by increasing the connectivity weight ($F = 5.181$, $p = 0.0041$, Fig. 4B).

To calculate network topology variation in response to glutamate treatment at incrementing concentrations, we applied two methods to analyze the network topology changes. First, to measure how the network density and size of the largest component change with increasing concentrations of glutamate, the functional networks at 21 DIV were constructed across a range of absolute thresholds (i.e., 0.5–10, in steps of 0.5; calculated for each network burst).The data show that treatment with 5, 10, 15, 20, and 25 μM glutamate increased the density of the functional network of the cortical neuronal cultures as compared with the no-glutamate condition across 0–5 thresholds (two-way ANOVA, $F = 1.10$, $p < 0.0001$, Fig. 4C). The difference in the size of the largest component between the no-glutamate condition and the 5 μM to 25 μM glu-

tamate treatments was significant across approximately 5–7.5 thresholds (two-way ANOVA, $F = 1.05$, $p < 0.0001$, Fig. 4D). Second, since the network density may affect the small-worldness, a range of proportional thresholds (i.e., 2–40% of the maximum network density, in steps of 2%) was used to construct the functional network at 21 DIV to calculate the small-worldness. Before glutamate exposure (0 μM), the small-worldness was above 1 for a wide proportion of the threshold range, demonstrating that the functional network of the neuronal cultures had a small-world organization topology. Glutamate treatment influenced the small-worldness of the neuronal cultures (two-way ANOVA, $F = 4.80$, $p < 0.0001$) (Fig. 4E).

4. Discussion

We investigated the effect of acute glutamate exposure on the activity parameters, functional connectivity, and functional network topology of cortical neuronal cultures using cross-covariance and graph theory. In addition, a shuffling procedure was applied to correct a possible error due to random spiking. Our results show that not only the activity parameters but also the connectivity and network topology of the cortical neuronal cultures could be influenced by glutamate.

Generally, neuronal cultures gradually demonstrate small-world [9] and "rich-club" [21] organizations during development without any external stimulation. Moreover, this small-world organization can be abolished [23] after 2 d of a glutamate-induced injury and enhanced with the administration of neuronal protection drugs [29].

In our study, we found that the similarity and connectivity weight between functional networks in a recording episode could be increased by acute glutamate treatment, and similar results were also reported in an *in vivo* study [13].We can infer from the increase in similarity that glutamate may be involved in the regulation of the communication between neuronal networks. The cross-covariance error of random spiking was corrected using a shuffling procedure; therefore, the higher the connectivity weight, the stronger the functional connection. An increase in connectivity weight suggests that the communication between neurons was enriched by the application of glutamate.

Moreover, the network density, size of the largest component, and small-worldness of cortical cultures were affected by glutamate exposure. The network density and size of the largest component could be enhanced by glutamate. This observation suggests that glutamate can increase the connections within a neuronal network. Although the small-worldness of the cortical culture was affected by glutamate, it remained above 1, indicating that the small-world organization of the neuronal cultures was not affected by glutamate.

Glutamate enhances the excitability of individual neurons. However, it is unknown how glutamate affects the global properties of a neuronal network, such as the functional connectivity. Using graph-theory measures of functional connectivity, we could measure the entire connectivity of a neuronal network to understand neuronal network functions, including the interaction of the functional structures of neurons and dynamic properties. In addition, our *in vitro* study advanced the understanding of the functional network organization, which may inspire future *in vivo* investigations.

Our study had some limitations, however. The 32 electrodes in our MEAs were not sufficient to record from all neurons in the neuronal network, and the missing information may have biased the small-world effect. Therefore, increasing the number and density of microelectrodes in future studies could provide information that is more accurate. In addition, separation of the network bursts into different types may be a more precise approach to analyze the data. Finally, in future studies, more network information such as modularity and hub measurements might reveal information that is more detailed.

The present study demonstrated that non-random properties of functional network in matured neuronal cultures were altered after acute glutamate treatment. Based on these results, we draw two main conclusions. First, to mitigate the influence of random spiking to the cross-covariance calculation, a shuffling procedure should be added in the connectivity weight evaluation. Second, the functional network of a cortical culture would increase in similarity, connectivity weight, density, and largest-component size. In addition, the small-world topology is altered after glutamate treatment. we propose this is due to a change in the excitatory-inhibitory balance that is caused by glutamate.

Acknowledgments

The authors thank CL Wang for cell culturing and data recording. Dr Duan Qing is highly appreciated for his efforts in editing this manuscript, including the syntax, grammar, and word usage.

Author contributions

Y Han and HM Zhu wrote the main manuscript and prepared Figs. 2–6. YW Zhao, YR Lang and HJ Sun cultured the neurons and prepared Fig. 1. P Zhang and JQ Han collected the data. LB Wang and J Zhou revised the manuscript. CY Wang managed the entire experiment. All authors reviewed the manuscript.

Conflicts of interest

None.

Funding

This work received the support of the National Key Research and Development Program of China (No.2017YFA0106100), National Key Research and Development Program of China (No.2016YFC1101303), National Natural Science Funds for Outstanding Young Scholar (No. 81622027) and Beijing NOVA Program of China (No. 2016B615)

Ethical approval

All animal experiments were performed under the guidelines published in the recommendations from the Declaration of Helsinki. The Institutional Animal Care and Use Committee (IACUC) of the Chinese Academy of Military Medical Science, Beijing, China, approved the animal experiments described in this study. All efforts were made to reduce the number of animals used.

References

[1] Aertsen AM, Gerstein GL. Evaluation of neuronal connectivity: sensitivity of cross-correlation. Brain Res 1985;340:341–54.
[2] Baruchi I, Ben-Jacob E. Towards neuro-memory-chip: imprinting multiple memories in cultured neural networks. Phys Rev E Stat Nonlin Soft Matter Phys 2007;75:050901.
[3] Beggs JM, Plenz D. Neuronal avalanches are diverse and precise activity patterns that are stable for many hours in cortical slice cultures. J Neurosci 2004;24:5216–29.
[4] Bettencourt LM, Stephens GJ, Ham MI, Gross GW. Functional structure of cortical neuronal networks grown *in vitro*. Phys Rev E Stat Nonlin Soft Matter Phys 2007;75:021915.
[5] Chiappalone M, Novellino A, Vajda I, Vato A, Martinoia S, van Pelt J. Burst detection algorithms for the analysis of spatio-temporal patterns in cortical networks of neurons. Neurocomputing 2005;65–66:653–62.
[6] Chiappalone M, Vato A, Berdondini L, Koudelka-Hep M, Martinoia S. Network dynamics and synchronous activity in cultured cortical neurons. Int J Neural Syst 2007;17:87–103.

[7] de la Rocha J, Doiron B, Shea-Brown E, Josic K, Reyes A. Correlation between neural spike trains increases with firing rate. Nature 2007;448:802–6.
[8] Defranchi E, Novellino A, Whelan M, Vogel S, Ramirez T, van Ravenzwaay B, Landsiedel R. Feasibility assessment of micro-electrode chip assay as a method of detecting neurotoxicity *in vitro*. Front Neuroeng 2011;4:6.
[9] Downes JH, Hammond MW, Xydas D, Spencer MC, Becerra VM, Warwick K, Whalley BJ, Nasuto SJ. Emergence of a small-world functional network in cultured neurons. PLoS Comput Biol 2012;8:e1002522.
[10] Gross GW, Rhoades BK, Azzazy HM, Wu MC. The use of neuronal networks on multielectrode arrays as biosensors. Biosens Bioelectron 1995;10:553–67.
[11] Harris KD, Csicsvari J, Hirase H, Dragoi G, Buzsaki G. Organization of cell assemblies in the hippocampus. Nature 2003;424:552–6.
[12] Humphries MD, Gurney K. Network 'small-world-ness': a quantitative method for determining canonical network equivalence. PLoS ONE 2008;3:e0002051.
[13] Kapogiannis D, Reiter DA, Willette AA, Mattson MP. Posteromedial cortex glutamate and GABA predict intrinsic functional connectivity of the default mode network. Neuroimage 2013;64:112–19.
[14] Khazipov R, Esclapez M, Caillard O, Bernard C, Khalilov I, Tyzio R, Hirsch J, Dzhala V, Berger B, Ben-Ari Y. Early development of neuronal activity in the primate hippocampus in utero. J Neurosci 2001;21:9770–981.
[15] Leinekugel X, Khazipov R, Cannon R, Hirase H, Ben-Ari Y, Buzsaki G. Correlated bursts of activity in the neonatal hippocampus *in vivo*. Science 2002;296:2049–52.
[16] Maccione A, Garofalo M, Nieus T, Tedesco M, Berdondini L, Martinoia S. Multiscale functional connectivity estimation on low-density neuronal cultures recorded by high-density CMOS micro electrode arrays. J Neurosci Methods 2012;207:161–71.
[17] Marom S, Shahaf G. Development, learning and memory in large random networks of cortical neurons: lessons beyond anatomy. Q Rev Biophys 2002;35:63–87.
[18] Morin FO, Takamura Y, Tamiya E. Investigating neuronal activity with planar microelectrode arrays: achievements and new perspectives. J Biosci Bioeng 2005;100:131–43.
[19] Raichman N, Ben-Jacob E. Identifying repeating motifs in the activation of synchronized bursts in cultured neuronal networks. J Neurosci Methods 2008;170:96–110.
[20] Rubinov M, Sporns O. Complex network measures of brain connectivity: uses and interpretations. Neuroimage 2010;52:1059–69.
[21] Schroeter MS, Charlesworth P, Kitzbichler MG, Paulsen O, Bullmore ET. Emergence of rich-club topology and coordinated dynamics in development of hippocampal functional networks *in vitro*. J Neurosci 2015;35:5459–70.
[22] Segev R, Baruchi I, Hulata E, Ben-Jacob E. Hidden neuronal correlations in cultured networks. Phys Rev Lett 2004;92:118102.
[23] Srinivas KV, Jain R, Saurav S, Sikdar SK. Small-world network topology of hippocampal neuronal network is lost, in an *in vitro* glutamate injury model of epilepsy. Eur J Neurosci 2007;25:3276–86.
[24] Sun JJ, Kilb W, Luhmann HJ. Self-organization of repetitive spike patterns in developing neuronal networks *in vitro*. Eur J Neurosci 2010;32:1289–99.
[25] Tang R, Pei W, Chen S, Zhao H, Chen Y, Han Y, Wang C, Chen H. Fabrication of strongly adherent platinum black coatings on microelectrodes array. Sci China Inf Sci 2014;57:1–10.
[26] Tang R, Zhang G, Weng X, Han Y, Lang Y, Zhao Y, Zhao X, Wang K, Lin Q, Wang C. *In vitro* assessment reveals parameters-dependent modulation on excitability and functional connectivity of cerebellar slice by repetitive transcranial magnetic stimulation. Sci Rep 2016;6:23420.
[27] Tateno T, Kawana A, Jimbo Y. Analytical characterization of spontaneous firing in networks of developing rat cultured cortical neurons. Phys Rev E Stat Nonlinear Soft Matter Phys 2002;65:051924.
[28] Teller S, Tahirbegi IB, Mir M, Samitier J, Soriano J. Magnetite-Amyloid-beta deteriorates activity and functional organization in an *in vitro* model for Alzheimer's disease. Sci Rep 2015;5:17261.
[29] Vincent K, Tauskela JS, Mealing GA, Thivierge JP. Altered network communication following a neuroprotective drug treatment. PLoS ONE 2013;8:e54478.
[30] Wagenaar DA, DeMarse TB, Potter SM. MeaBench: a toolset for multielectrode data acquisition and on-line analysis. In: Proceedings of the 2nd international IEEE EMBS conference neural engineering Arlington; 2005.
[31] Wagenaar DA, Pine J, Potter SM. An extremely rich repertoire of bursting patterns during the development of cortical cultures. BMC Neurosci 2006;7:11.
[32] Watts DJ, Strogatz SH. Collective dynamics of 'small-world' networks. Nature 1998;393:440–2.
[33] Yao H, Rongyu T, Jin Z, Qiuxia L, Zhiqiang L, Weizhen C, DuanCuimi WChunlan, Changyong W. The design and fabrication of microelectrode array (MEA) and multichannel electrophysiology system. J Biomed Eng Res 2012:214–19.